THz-pump – THz-probe spectroscopy of semiconductors at high field strengths

Matthias C. Hoffmann,[1,*] János Hebling,[2] Harold Y. Hwang,[1] Ka-Lo Yeh,[1] and Keith A. Nelson[1]

[1]*Massachusetts Institute of Technology*

[2]*Department of Physics,University of Pécs, Hungary*

(Dated: February 3, 2022)

Abstract

Pumping n-type GaAs and InSb with ultrafast THz pulses having intensities higher than 150 MW/cm^2 shows strong free carrier absorption saturation at temperatures of 300 K and 200 K respectively. If the energy imparted to the carriers exceeds the bandgap, impact ionization processes can occur. The dynamics of carrier cooling in GaAs and impact ionization in InSb were monitored using THz-pump/THz probe spectroscopy which provides both sub-bandgap excitation and probing, eliminating any direct optical electron-hole generation that complicates the evaluation of results in optical pump/THz probe experiments.

PACS numbers: 78.47.J-,71.55.Eq, 72.20.Ht,72.20.Jv,42.65.Re

INTRODUCTION

The study of hot carrier effects plays a central role in the advancement of semiconductor science. Properties of hot carriers are influenced both by the interaction between carriers and that between the lattice and the carriers. Information about these scattering processes, which determine high-field transport phenomena in semiconductors, is highly valuable because they constitute the basis of many ultrafast electronic and optoelectronic devices. With the advent of ultrafast lasers, the dynamics of hot carrier effects have been studied intensively on the picosecond and femtosecond timescales. In a typical experiment, new carriers are generated by an optical pump beam with a photon energy, ϵ_{ph}, above the bandgap, ϵ_g, of the semiconductor. The newly generated electrons and holes share the excess energy ϵ_{ph}-ϵ_g in a ratio inversely proportional to their effective masses and subsequently undergo cooling processes mediated by carrier-carrier and carrier phonon scattering. The dynamics of these cooling processes can then be monitored by short probe pulses of appropriate wavelength. This technique has successfully been applied to a large range of semiconductors and semiconductor nanostructures and a substantial amount of basic information was collected in this way [1].

With photo excitation, an equal number of electrons and holes are created. Hence, most ultrafast optical studies are performed in the presence of a plasma containing both types of carriers. Experimental observations can be complicated by the dynamics that involve both electrons and holes. When properties like the coupling to the phonons and carrier-carrier scattering are different for the two components and the density of carriers is time dependent, a direct interpretation of the experimental data is further hindered. Near-IR pump/THz probe experiments also suffer from this shortcoming [2, 3, 4].

In this article we report results from THz-pump/THz-probe measurements used to monitor the inter- and intra-valley dynamics of extremely hot free electrons in GaAs and the generation of new carriers by impact ionization in InSb. THz electric field strengths up to 150 kV/cm at the surface of the semiconductor were achieved. Fields of this magnitude and correspondingly hot electrons are present inside different fast semiconductor devices like Gunn-diodes and avalanche photo diodes. Electron heating by the THz pulse and strong intervalley scattering cause a large fraction of the electrons to scatter out from the initial lowest energy conduction band valley into side valleys. Based on a rough estimate, electrons

can reach an average energy on the order of 1 eV. Since free-carrier absorption is proportional to carrier concentration and carrier mobility, and because different conduction band valleys usually have significantly different mobilities from each other, the change in the distribution of electrons amongst the different valleys causes a change in THz absorption. This behaviour has been observed with nanosecond transmission experiments with field strengths up to 10 kV/cm [5] and was monitored via the absorption of a delayed probe THz pulse.

EXPERIMENTAL TECHNIQUE

The experimental setup shown in Figure 1 was used to elucidate the dynamics of hot carriers in doped semiconductors. We generated single-cycle THz pulses by optical rectification of pulses from a femtosecond laser using the tilted-pulse-front method [6]. This technique uses a tilted intensity front of a femtosecond laser pulse to achieve velocity matching of the phonon polaritons inside lithium niobate and the femtosecond laser light [7]. The tilted pulse front enables the use of high optical pulse energy to build up large THz field amplitudes while averting unwanted nonlinear optical effects. THz pulse energies greater than 10 μJ can be achieved using this method [8]. Because the angle of the pulse front tilt can be arbitrarily chosen, the method can also be adapted for other materials and wavelengths [9]. For our experiments a regeneratively amplified titanium sapphire laser system with 6 mJ pulse energy and 100 fs pulse duration at a repetition rate of 1 kHz was used. The optical beam was split using a 10:90 beamsplitter into two parts that were recombined under a small angle at the same spot on the grating. The 10% part was passed through a chopper wheel (not shown in figure) and was used to generate the THz probe. The 90% part was variably delayed, and used to generate the THz pump pulse. The single-cycle THz pulses were focused onto the sample using a 90-degree off-axis parabolic mirror pair with 190 and 75 mm focal lengths. The ratio of focal lengths allows us to reduce the beam diameter at the sample to 1 mm. Another off-axis parabolic mirror pair with focal lengths of 100 and 190 mm was used to image the sample plane onto the ZnTe detector crystal for electro-optic sampling of the THz field using balanced detection and a lock-in amplifier [10]. Because larger than 2 π phase shifts are routinely observed with thicker ZnTe crystals, we used a ZnTe compound detector with an active layer of 0.1 mm and a total thickness of 1.1 mm to ensure the linearity of the detected signal and to eliminate THz pulse reflections within

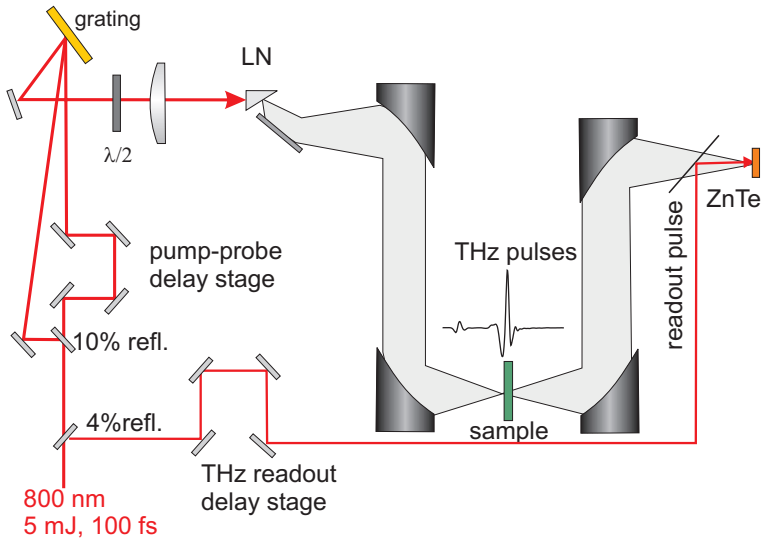

FIG. 1: (color online) Schematic illustration of the experimental setup. Collinear THz pulses are generated by tilted pulse front excitation in LiNbO3 (LN) and detected electro-optically. See text for details.

the crystal [11]. Selective chopping of the probe beam provided excellent suppression of the pump pulse. Spectral analysis of our THz pump-probe results was conducted in the 0.2 to 1.6 THz range where the spectral amplitude was sufficiently high. A pair of wiregrid polarizers was used to attenuate the THz pulses for intensity-dependent studies. We measured the THz fields $E(t)$ that reached the ZnTe crystal with and without the sample in the beam path and calculated the effective absorption coefficient

$$\alpha_{\text{eff}} = -\frac{1}{d}\ln\left(T^2 \cdot \frac{\int_0^{t_{\max}} E_{\text{sam}}^2(t)dt}{\int_0^{t_{\max}} E_{\text{ref}}^2(t)dt}\right) \tag{1}$$

where d is the sample thickness, t_{max} is the time window of the measurement and T is a factor accounting for reflection losses at the sample surfaces. The quantity α_{eff} is equivalent to the energy absorption coefficient averaged over our bandwidth. Referencing the recorded data against the electric field measured without the sample enables us to compensate nonlinear effects within the LN generation crystal to a large degree. Only in a time interval of ± 1 ps around the overlap time of the pump and probe does the data quality become unreliable.

The same setup can be reconfigured for intensity dependent transmission studies by

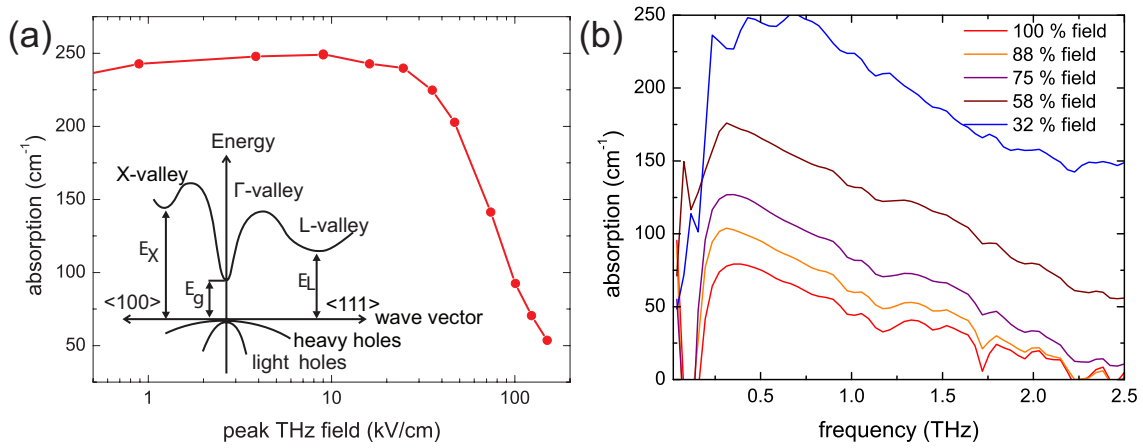

FIG. 2: (color online) (a) Average THz absorption in n-type GaAs for peak fields between 1 and 150 kV/cm, the inset shows the simplified band structure of GaAs. (b) Frequency resolved absorption spectra at selected field strengths.

simply blocking the optical pulse used to generate the THz probe beam, chopping the portion used to create the THz pump, and changing the angle between the first and second THz wiregrid polarizers to vary the intensity of the THz pump pulse.

HOT ELECTRON DYNAMICS IN N-TYPE GAAS

Saturation of free-carrier absorption

Free-carrier absorption in the THz range, which can be described by the Drude model, is readily observed in bulk doped semiconductors [2, 12]. Linear THz-TDS measurements of n-type GaAs revealed the Drude behavior of GaAs that is dependent on both the doping concentration and mobility of the sample.

In order to investigate free-carrier absorption in strong THz fields, nonlinear THz transmission measurements were performed on a 450 μm thick, n-type GaAs wafer with a carrier concentration of 8×10^{15} cm^{-3} at 300 K. THz pulse energies and peak fields of up to 2 μJ and 150 kV/cm respectively were used. Figure 2a shows the observed averaged THz absorption between 0.35 and 1.5 THz for a range of peak fields. At THz fields smaller than 10 kV/cm, the absorption approaches the values obtained in linear THz transmission experiments conducted using a spectrometer with photoconductive switches.

Starting at peak fields of 30 kV/cm, we observe a drastic drop in the absorption coefficient.

At fields larger than 100 kV/cm, the saturation effect appears to level off slightly.

Figure 2b shows the corresponding absorption spectra for various selected field strengths above 50 kV/cm. Even though the overall spectrum does not change in shape, the absorption drops uniformly over a broad frequency range.

The decrease in absorption can be explained qualitatively by the change of carrier mobility due to the acceleration of the free electrons in the conduction band by the electric field of the THz pulse. Taking into account energy relaxation during the 1 ps pump pulse duration, we estimate the average carrier energy just after the pump pulse to be in the 0.5–1.3 eV range, exceeding the energy necessary for carriers to cross into the side valleys. These values are consistent with Monte-Carlo simulations that show that electrons can reach ballistic velocities of up to 10^8cm/s within 30 fs in external electric fields [13]. The ballistic acceleration competes with phonon scattering processes after 30 fs, leading to an average heating of the electron gas on a timescale faster than the THz pulse duration of 1 ps.

Electrons with these high energies can scatter into satellite valleys (L and X) of the conduction band which have an energy separation from the bottom of the zone center (Γ-valley) of 0.29 eV and 0.48 eV respectively. The effective mass at the zone center is 0.063 m_0 leading to high mobility and high THz absorption. The density of states effective mass in the side valleys is much higher (0.85 m_0) resulting in much smaller mobility.

In addition to the difference in mobilities among the initial and side valleys, the nonparabolicity of the valleys can also result in a decrease in mobility and a concomitant decrease in THz absorption that accompanies the increase in carrier kinetic energy within a single valley. Energy-dependent effective mass and nonparabolicity parameters reported for GaAs [13] indicate that adding 0.3 eV of kinetic energy to electrons in the lowest-energy valleys reduces their THz absorption by 2/3.

Time resolved absorption measurements

With simple intensity dependent transmission measurements we are unable to observe relaxation of the excited carriers back into the Γ valley after the strong heating of the electron gas by the THz pulse. This cooling process can only be observed via time resolved measurements. In particular, different relaxation times are expected for inter- and intra-valley relaxations, necessitating the use of the THz-pump/THz-probe technique described

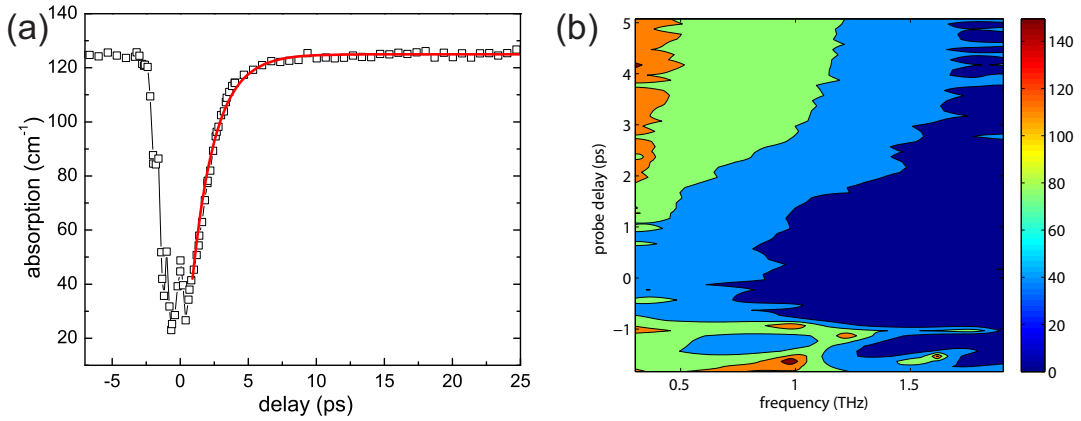

FIG. 3: (color online): (a) The recovery of the absorption as a function of THz probe delay after the arrival of a strong THz pump pulse at t=0. (b) Frequency dependent absorption coefficient (cm-1) as a function of probe delay times, revealing the relaxation of the excited carriers back to their equilibrium Drude-like behavior 5 ps after the arrival of the pump pulse.

in the earlier experimental section.

Figure 3a shows the time resolved absorption upon THz excitation of the n-type GaAs sample. The equilibrium frequency-averaged absorption of 125 cm^{-1} drops below 30 cm^{-1} immediately after the arrival of the THz pump pulse. The drop in absorption occurs on the same timescale as the time resolution provided by our pulses. A complete recovery of the absorption is reached after 7 ps. An exponential fit of the absorption (solid line in Figure 3a) yields a carrier relaxtion time of $\tau_r = 1.9$ ps. In the frequency domain, (shown in Figure 3b), we observe a slow recovery of the Drude absorption until the initial absorption is restored. The observation that the relaxation time from the L-valley is much larger than the scattering time into it can be explained by the fact that it is governed by the relaxation rate from the upper Γ state to the lower Γ state, and only those carriers in the lower Γ state are allowed to contribute to the signal. Rate equations for the intervalley scattering have been employed by Stanton [14].

Similar to the field dependent nonlinear transmission measurements shown in Figure 2a, the time resolved absorption spectra in our pump-probe measurements can be fit to a simple Drude-model. Keeping the carrier concentration at the constant value obtained from Hall measurements by the manufacturer, we can extract an averaged effective mass. The result of

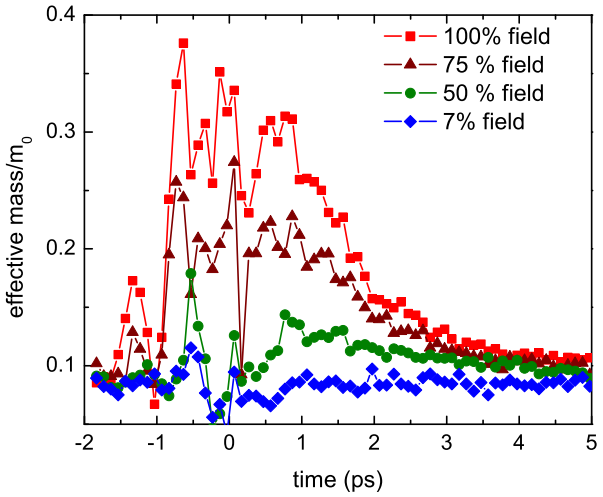

FIG. 4: (color online): Average effective mass, relative to the electron mass, obtained from Drude-fits to the absorption spectra for different pump field strengths.

the time evolution of this quantity for different pump strengths is shown in Figure 4. At high field strengths the average effective mass exceeds a value of 0.3 $m_0$suggesting that a sizeable fraction of the carriers is scattered into the side valleys with higher mass. Qualitatively we also observe a rise in the effective scattering time, although the data quality does not allow us to make quantitative conclusions.

THZ-INDUCED IMPACT IONIZATION IN INSB

Indium antimonide (InSb) has the highest electron mobility and saturation velocity of all known semiconductors, enabling the fabrication of transistors with extremely high switching speeds [15]. The elucidation of carrier dynamics in InSb on the ultrashort timescale is hence of great fundamental and technological relevance. The material is a direct semiconductor with a bandgap of 170 meV at room temperature [16], making it well-suited for applications in infrared sensors covering the wavelength range from 1 μm to 5 μm [17].

Impact ionization by high electric fields is a well known phenomenon in InSb [18]. The effect is determined by the probability that an electron will gain enough energy from the driving field to cross the ionization threshold. This is usually observed at relatively low DC fields of several hundred V/cm where avalanche effects play an important role. Strong THz fields can directly achieve impact ionization on the picosecond time scale [19] while avoiding

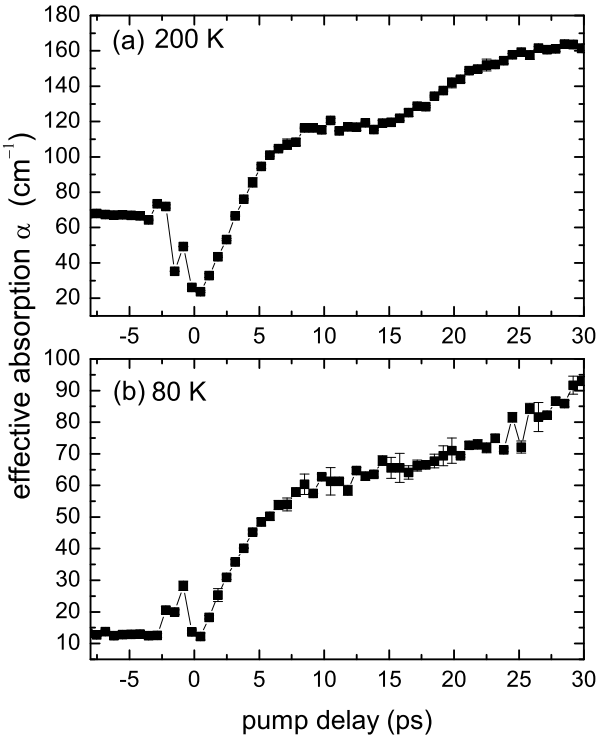

FIG. 5: Time-resolved THz absorption of doped InSb at 200K and 80K after excitation by a 2 μJ THz pulse.

additional experimental complications by the use of photons with energies well below the bandgap.

Because of the small bandgap, undoped InSb has a high intrinsic carrier concentration of 2×10^{16} cm^{-3}at room temperature. Even at 200 K the absorption still exceeds 200 cm^{-1} at frequencies below 1 THz. At temperatures of 80K, the intrinsic carrier concentration is on the order of 10^{9}cm^{-3}and the remaining carrier concentration is dominated by impurities.

In intensity dependent transmission measurements at high intrinsic carrier concentrations (200 K), we observe a behavior similar to that of GaAs (Figure 2a) with a drop in average absorption to 50% of the low intensity value. At low carrier concentration of 2×10^{14} cm^{-3} (80 K) we observe a small rise in THz absorption at high fields in transmission measurements, similar to the results reported in [19], hinting at new carrier generation by the impact ionization process.

In order to understand the dynamics of carrier heating and subsequent impact ionization we carried out pump-probe measurements by the method described above. Figure 5 shows time resolved absorption data for n-type Te-doped InSb with a carrier concentration of

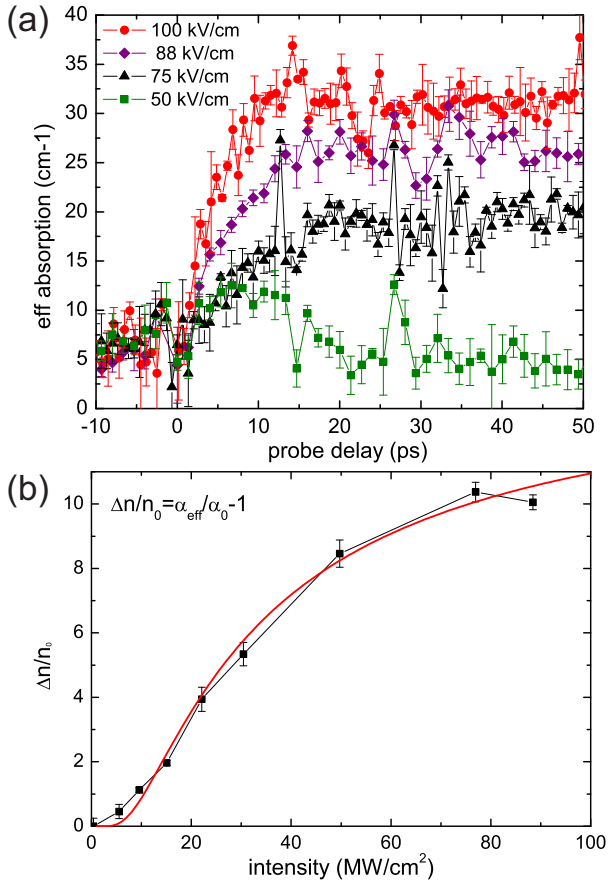

FIG. 6: (color online) (a) time-resolved averaged absorption (0.2-1.6 THz) in undoped InSb at 80K for various fields (b) intensity dependent average absorption for the doped sample 35 ps after the THz excitation, the solid line is a fit to Eq. (2)

2.0×10^{15} cm^{-3}at 77 K. The mobility as specified by the manufacturer was 2.5×10^{5} cm^2/Vs. The THz fields were polarized parallel to the (100) axes of the crystals. At sample temperatures of 200 K and 80 K the absorption increases by roughly the same amount (80-90 cm^{-1}) after 30 ps. At 200 K, there is an initial dip in absorption before a subsequent rise after a few ps, confirming the findings in our transmission measurements. No such initial decrease is observed at 80 K. The difference in the early time absorption behavior is due to the opposing effects of impact ionization and carrier heating, both caused by the THz pump pulse. Electron heating leads to a decrease in mobility due to the strong non-parabolicity in the conduction band of InSb [20] and scattering into side valleys with lower mobility [21], similar to the case of GaAs discussed in the previous section.

Further pump-field dependent experimental results shown in Figure 6a indicate no ob-

servable absorption increase for single-cycle THz pulses with peak electric fields lower than 75 kV/cm in nominally undoped InSb with a carrier concentration lower than $5\times10^{14}\mathrm{cm}^{-3}$at 77K.

The threshold electric field in this case should be distinguished from that obtained in prior static or quasi-static measurements [22]. From a simple model we were able to extrapolate that the peak field required for impact ionization by the single-cycle THz pulse excitation is a factor of two larger than in the static field case [23]. This difference can be attributed to the significantly shorter peak pulse duration compared to the momentum relaxation time in InSb.

The intensity dependence of impact ionization by 40 ns far-infrared pulse has been observed by Ganichev [24] using photoconductive measurements. In this case, the electron concentration change $\Delta\mathrm{n}/\mathrm{n}_0$ by impact ionization could be modeled using the Fokker-Planck equation, leading to a dependence on the applied electric field E given by

$$\frac{\Delta n}{n} = A \exp\left(\frac{-E_0^2}{E^2}\right) \tag{2}$$

where A is a proportionality constant.

To check the validity of equation (2) in the regime of very short pulses with high energy, we performed a series of intensity dependent pump probe measurements with the probe delay held constant at 35 ps after the arrival of pump. Figure 6b shows the intensity dependent average THz absorption for the doped InSb at 80 K. We observe a saturation of the new carrier generation at high pump fluencies. The solid line shows fit to the experimental data using equation (2) with parameter values $A = 14.5$ and E_0=104 kV/cm. The parameter E_0 is a characteristic field that gives electrons enough energy to create an electron hole pair. While the fit gives adequate agreement with Eq. 2, the critical field E_0 is roughly 2 orders of magnitude higher than that observed in Ref. [24] for 40 ns THz laser pulses. This discrepancy can only be understood taking into account the fundamentally nonequilibrium carrier heating induced by the single cycle THz pulse as opposed to the quasi-cw AC field case in previous experiments.

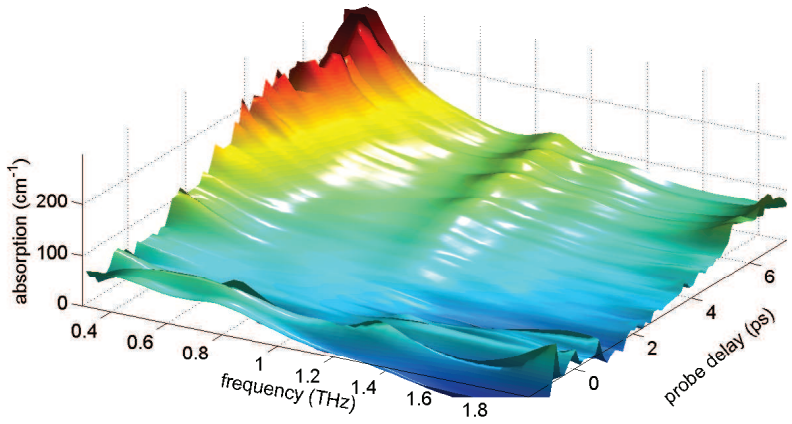

FIG. 7: (color online) The frequency dependent absorption coefficient of InSb as a function of frequency for probe delays up to 7 ps at a temperature of 200 K.

Plasma-Lattice interaction

A distinct absorption peak at 1.2 THz in the undoped sample and a weak feature that indicates a similar peak in the doped sample were observed. Figure 7 illustrates the appearance of this peak for pump-probe delay times up to 7 ps in the doped sample at 200 K. The evolution of the low frequency Drude behavior is clearly separated from the phonon mediated peak at 1.2 THz.

The amplitude – but not the frequency - of the peak is highly intensity dependent, and appears to approach its asymptotic value just above 50% of the maximum THz intensity. This behavior of this peak suggests that its origin is lattice vibrational rather than electronic. Polar optical phonon scattering is well known as the dominant energy loss mechanism for hot electrons in InSb [25]. The main channel of energy loss is through the emission of LO phonons with a frequency of 5.94 THz. These phonons decay into acoustic modes through both anharmonic coupling and the second-order electric moment of the lattice [26]. A series of sum- and difference phonon peaks between 1 to 10 THz has been observed and assigned in the far-infrared spectrum of InSb [27]. At very low THz fields produced by a photoconductive antenna, we were also able to observe some of these weak absorption peaks in the undoped sample. The phonon frequency assignments reported in [27] indicate a 1.2 THz difference frequency between the LO and LA modes at the zone boundary. The drastic change in the absorption coefficient of the difference phonon peak is the result of large changes in phonon

populations that can be attributed to the energy transfer from hot electrons generated by the THz pump pulse. Monte-Carlo simulations [28] have shown that substantial phonon population changes can occur even at comparatively low DC fields on picosecond timescales.

CONCLUSION

We have demonstrated the ability to accelerate free carriers in doped semiconductors to high energies by single cycle THz pulses. At the same time, THz probing enables the monitoring of the free carrier absorption on the picosecond timescale. For GaAs we are able to observe that a fraction of carriers undergo intervalley scattering, leading to a drastic change in effective mass. In the case of InSb, the carrier energy can exceed the impact ionization threshold, leading to an increase of carrier concentration of about one order of magnitude. In this material we are able to observe the energy exchange between the hot electrons and the lattice, leading to changes in population of the LO phonon. Monte-Carlo simulations are needed for a more in-depth understanding of the interplay between hot electrons and the lattice, in which effects like impact ionization, intervalley- and polar optical phonon scattering and changes in phonon population are taken into account. Experimentally, a broader probe bandwidth exceeding 2 THz will enable us to monitor the phonon dynamics directly. With even higher THz fields we should be able to achieve impact ionization in higher band-gap materials like Germanium or GaAs allowing us to understand these highly nonlinear transport phenomena without experimental complications due to avalanche effects or multiphoton absorption.

This work was supported in part by ONR under Grant No. N00014-06-1-0463.

* mch@mit.edu

[1] J. Shah, *Ultrafast Spectroscopy of Semiconductors and Semiconductors Nanostructures* (Springer, 1999), 2nd ed.

[2] M. van Exter and D. Grischkowsky, Physical Review B **41**, 12140 (1990).

[3] S. E. Ralph, Y. Chen, J. Woodall, and D. McInturff, Phys. Rev. B **54**, 5568 (1996).

[4] M. C. Nuss, D. H. Auston, and F. Capasso, Phys. Rev. Lett. **58**, 2355 (1987).

[5] A. Mayer and F. Keilmann, Phys. Rev. B **33**, 6962 (1986).

[6] J. Hebling, G. Almasi, I. Kozma, and J. Kuhl, Optics Express **10**, 1161 (2002).

[7] T. Feurer, N. S. Stoyanov, D. W. Ward, J. Vaughan, E. R. Statz, and K. A. Nelson, Annu. Rev. Mater. Res. **37**, 317 (2007).

[8] K.-L. Yeh, M. C. Hoffmann, J. Hebling, and K. A. Nelson, Appl. Phys. Lett. **90**, 171121 (2007).

[9] M. C. Hoffmann, K.-L. Yeh, J. J. Hebling, and K. A. Nelson, Optics Express **15**, 11706 (2007).

[10] Q. Wu and X.-C. Zhang, Appl. Phys. Lett. **67**, 3523 (1995).

[11] D. Turchinovich and J. I. Dijkhuis, Opt. Commun. **270**, 96 (2007).

[12] P. G. Huggard, J. A. Cluff, G. P. Moore, C. J. Shaw, S. R. Andrews, S. R. Keiding, E. H. Linfield, and D. A. Ritchie, J. Appl. Phys. **87**, 2382 (2000).

[13] H. Shichijo and K. Hess, Phys. Rev. B **23**, 4197 (1981).

[14] C. J. Stanton and D. W. Bailey, Phys. Rev. B **45**, 8369 8377 (1992).

[15] T. Ashley, A. Barnes, L. Buckle, S. Datta, A. Dean, M. Emery, M. Fearn, D. Hayes, K. Hilton, R. Jefferies, et al., in *Solid-State and Integrated Circuits Technology, 2004. Proceedings. 7th International Conference* (IEEE Press, Beijing, 2004), vol. 3, pp. 2253 – 2256.

[16] C. L. Littler and D. G. Seller, Appl. Phys. Lett. **46**, 986 (1985).

[17] D. G. Avery, D. W. Goodwin, and M. A. E. Rennie, J. Sci. Instrum. **34**, 394 (1957).

[18] C. L. Dick and B. Ancker-Johnson, Phys. Rev. B **5**, 526 (1972).

[19] H. Wen, M. Wiczer, and A. M. Lindenberg, Phys. Rev. B **78**, 125203 (2008).

[20] X. M. Weng and X. Lei, Phys. Stat. Solid. B **187**, 579 (1995).

[21] J. Hebling, M. C. Hoffmann, H. Y. Hwang, K.-L. Yeh, and K. A. Nelson, in *Ultrafast Phenomena XVI*, edited by P. Corkum, S. de Silvestri, K. A. Nelson, E. Riedle, and R. W. Schoenlein (Springer, 2008).

[22] R. Asauskas, Z. Dobrovolskis, and A. Krotkus, Soviet Physics Semiconductors **14**, 1377 (1980).

[23] M. C. Hoffmann, J. Hebling, H. Y. Hwang, K. L. Yeh, and K. A. Nelson, Phys. Rev. B **79**, 161201(R) (2009).

[24] S. D. Ganichev, A. P. Dmitriev, S. A. Emel'yanov, Ya, V. Terent'ev, I. D. Yaroshetskii, and I. N. Yassievich, Sov. Phys. JETP **63**, 256 (1986).

[25] E. M. Conwell, *High Field Transport in Semiconductors* (Academic Press, New York, 1967).

[26] D. Ferry, Phys. Rev. B **9**, 4277 (1974).

[27] E. S. Koteles, W. R. Datars, and G. Dolling, Phys. Rev. B **9**, 572 (1974).

[28] R. Brazis and R. Raguotis, Opt. Quant. Electron. **40**, 249 252 (2008).